

## THEORETICAL DISCHARGE CURVES FOR NICKEL HYDROXIDE

John W. Weidner  
Department of Chemical Engineering  
University of South Carolina  
Columbia, SC 29208

Paul Timmerman  
Jet Propulsion Laboratory  
California Institute of Technology  
Pasadena, CA 91109

### ABSTRACT

Discharge curves for the nickel hydroxide electrode are simulated assuming resistances due to diffusion of protons and conduction of electrons through the active nickel hydroxide film as well as charge-transfer resistance at the film/electrolyte interface contribute to the polarization losses of the electrode. Previous models which have combined these three resistances into a pseudocharge-transfer resistance predict discharge curves which are higher and flatter than experimental data, and material utilization which is unrealistically high. The present model predicts realistic trends as a function of discharge rates. In addition, the governing equations have been solved analytically which allows the model of the active film to be integrated into our battery models.

### INTRODUCTION

Battery models that can predict the effect of operating conditions on battery life and performance are extremely valuable to battery users and manufacturers. Model predictions can provide quality assurance that the batteries being manufactured are of consistently high quality, and provide indicators well in advance of failure so that steps can be taken to adjust operating condition and prolong battery life. In addition, a variety of design parameters can be investigated to aid an electrode development program.

Theoretical discharge curves have been generated by a number of investigators [1]—[5] using a one-dimensional, macrohomogeneous model. The spatial dimension of interest is in the direction perpendicular to the current collectors, and therefore the polarization loss across the  $\text{NiOOH}/\text{Ni}(\text{OH})_2$  active film is assumed to be due solely to charge-transfer resistance. Although these models reveal the importance of transport limitations in the electrolyte phase, they predict nickel electrode potentials as a function of time which are larger and more constant than experimental data. They also predict material utilization on discharge which is unrealistically high. Sinha [10] developed a model of a porous electrode in which the solid active material was described using semiconductor theory. This model, however, contains many parameters that can not be obtained experimentally.

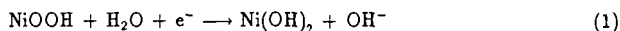
Experimentally it has been suggested that proton diffusion and ohmic drop in the active material may contribute appreciably to overall polarization losses [6]—[8]. Two dimensional,

macrohomogeneous models have been developed to account for the diffusion of protons in the active nickel hydroxide film [9] and diffusion coupled with electronic resistance of the film [11]. One of the rationals for including variable electronic resistance in the later model [11] is that the nickel hydroxide is an electrical insulator in the reduced state and a conductor in the oxidized state. The drawback of these models is that the solution procedure requires a large amount of computer memory and computational time.

In this paper, an analytical solution is given which accounts for proton diffusion and variable electronic conductivity in the film. This solution can be used in conjunction with a one-dimensional, macrohomogeneous model to achieve the results obtained by Mao *et al.* [11], but with considerably less computer power. In addition, the analytical solution can be used to simulate electroanalytical techniques in order to extract kinetic, transport, and electronic resistance parameters from experimental data.

## MATHEMATICAL MODEL

The discharge reaction at the nickel electrode is generally expressed as



Proton diffusion into the bulk of the solid phase makes it possible for this reaction to continue at the film/electrolyte interface. The kinetic expression given by previous investigators [5, 11] is used to relate the current to the potential driving force and proton concentration at this interface. For a constant current discharge, this expression can be written in dimensionless form as

$$1 = I_0 \left[ (1 - \theta_s) e^{\alpha_s \Phi_s} - \theta_s e^{-\alpha_s \Phi_s} \right] \quad (2)$$

where  $\theta_s$  is the state-of-charge at the film/electrolyte interface and is related to the proton concentration at this surface by

$$\theta_s = 1 - C_s(1 - \theta^0) \quad (3)$$

and  $\Phi_s$  is the dimensionless potential driving force at the surface defined as

$$\Phi_s = \frac{F}{RT}(\phi_s - U_{\text{ref}}) \quad (4)$$

The dimensionless potential driving force, therefore, is the potential drop across the film/electrolyte interface relative to a reference potential ( $U_{\text{ref}} = 0.440$  V versus SHE which is the open circuit potential for  $\text{Ni(OH)}_2$  at a degree of discharge of 0.5 in 31% KOH). (See the notation section and Table 1 for a complete list of variable and parameter definitions, respectively.)

In order to obtain  $C_s$ , the concentration profile of protons in the nickel hydroxide film must be obtained as a function of time. It is assumed that the proton concentration in the film is governed by the time-dependent, one-dimensional diffusion equation. In dimensionless form this equation can be written as

$$\frac{\partial C}{\partial \tau} = \frac{\partial^2 C}{\partial Y^2} \quad (5)$$

The initial proton concentration is uniform, the proton concentration gradient is zero at the film/substrate interface ( $Y = 0$ ), and the concentration gradient is proportional to the current at the film/electrolyte interface ( $Y = 1$ ). The initial and boundary conditions can be written as:

$$(5a) \quad \tau = 0; \quad C = 1$$

$$(5b) \quad Y = 0; \quad \frac{\partial C}{\partial Y} = 0$$

$$(5c) \quad Y = 1; \quad \frac{\partial C}{\partial Y} = \frac{1}{D(1-\theta^0)}$$

The Laplace transform of equation 5 is taken with respect to  $\tau$ , the resulting ordinary differential equation for the transformed concentration is solved, and the solution is inverted back to the time domain resulting in

$$C(Y, \tau) = 1 + \frac{1}{D(1-\theta^0)} \left[ \tau + 2 \sum_{k=1}^{\infty} \frac{(-1)^k \cos(k\pi Y)}{k^2 \pi^2} (1 - e^{-k^2 \pi^2 \tau}) \right] \quad (6)$$

In order to obtain the applied potential, ohm's law must be integrated from the conducting substrate ( $Y = 0$ ) to the electrolyte ( $Y = 1$ ) giving the following expression at room temperature.

$$\text{applied potential (mV vs SHE)} = 440 + 25.7 \left[ \Phi_s + \frac{1}{\Theta} \int_0^1 \frac{dY}{\sigma(Y, \tau)} \right] \quad (7)$$

where

$$\sigma(Y, \tau) = \exp \left[ -24.45 (1 - \theta^0)^4 C^4 \right] \quad (8)$$

Note that for a constant current discharge

$$\text{degree of discharge} = (1 - \theta^0) + \tau/D \quad (9)$$

## RESULTS AND DISCUSSION

Figure 1 shows the effect of discharge rate on discharge curves for nickel hydroxide. The term  $c/n$  is the current which causes the electrode to completely discharge in  $n$  hours. Each curve was obtained by solving equation 6 at  $Y = 1$ , solving equation 2 for  $\Phi_s$ , obtaining the applied potential from equation 7, and then repeating these steps at successive points in time. The values used to calculate the dimensionless parameters given in Figure 1 are listed in Table 2.

The convergence of the series in equation 6 was accelerated using Richardson extrapolation [13] and a binomial averaging algorithm [14] for  $Y = 1$  and  $Y \neq 1$ , respectively. Equation 7 was integrated numerically using Simpson's rule, and Newton's method was used to obtain  $\Phi_s$  from equation 2.

Three features which are observed experimentally are also seen in the theoretical discharge curves shown in Figure 1. The first feature is the curvature observed during the early stages of discharge (degree of discharge  $< 0.05$ ). The other two features seen in Figure 1 are the potential dependence of the middle plateau and the abrupt drop in the potential as a function of discharge rate. This abrupt drop in potential is a critical characteristic of the discharge curve since the electrode loses its energy producing capability at this point and the remaining capacity can not be utilized.

It is unclear from Figure 1 what the relative contributions of mass-transfer, ohmic, and kinetic resistances are to the observed polarization losses. Figures 2-4 were generated at a discharge rate of  $c/2$  in order to isolate the individual resistances, and determine their effect on the discharge

curves. The polarization losses seen in Figure 2 are due solely to kinetic resistance since  $\mathcal{D}$  and  $\Theta$  were increased by many orders of magnitude. Kinetic resistance alone can not account for two of the three trends observed experimentally. Namely, utilization is not affected by kinetic limitations since approximately 100% utilization is observed even when kinetic resistance (or discharge rate) is increased two orders-of-magnitude from the base case. The curvature of the discharge curves is also lost as kinetic resistance is increased relative to discharge time. This observation suggests that kinetic resistance may be a small contributor to the overall polarization losses observed in a nickel hydroxide electrode.

The polarization losses seen in Figure 3 are due solely to the mass-transfer resistance of protons through the active nickel hydroxide film. The same trends seen in Figure 1 are observed in Figure 3. Consequently, diffusion alone could account for curvature during the early stages of discharge, and a middle plateau and material utilization which are functions of discharge rate.

Figure 4 shows the polarization losses due to ohmic resistance. Curvature is seen at the early stages of discharge, and material utilization decreases as ohmic resistance relative to discharge time increases. However, a four order-of-magnitude increase in ohmic resistance did not affect utilization as much as a one order-of-magnitude increase in mass-transfer resistance did. In addition, polarization losses at the midpoint of discharge are not a function of discharge rate. As with kinetic resistance, ohmic resistance alone can not account for all the trends observed from experimental discharge curves.

## CONCLUSIONS

Discharge curves for the nickel hydroxide electrode were simulated assuming resistances due to diffusion of protons and conduction of electrons through the active nickel hydroxide film as well as charge-transfer resistance at the film/electrode interface contribute to the polarization losses of the electrode. The model was able to predict realistic trends as a function of discharge curves. The results suggest that polarization losses due to diffusional limitations of protons is a critical factor in determining the shape of the discharge curve. Variable electronic resistance has a noticeable effect on the discharge curve but it alone can not account for all the observed trends. Charge-transfer resistance is insignificant relative to ohmic and mass-transfer resistance.

## NOTATION

$c_{H+}$	proton concentration, mol/cm <sup>3</sup>
$c_{H+}^0$	proton concentration, mol/cm <sup>3</sup>
$c_{Ni}$	concentration of nickel sites, mol/cm <sup>3</sup>
$C$	dimensionless proton concentration, $c_{H+}/c_{H+}^0$
$C_s$	dimensionless proton concentration at $Y = 1$
$D_{H+}$	diffusion coefficient for protons, cm <sup>2</sup> /s
$f$	$F/RT$ , V <sup>-1</sup>
$F$	Faraday's constant, C/equiv
$i$	current density, A/cm <sup>2</sup>
$i_0$	exchange current density, A/cm <sup>2</sup>
$l$	thickness of the nickel hydroxide layer, cm
$n$	hours required for complete discharge, hr
$R$	gas constant, J/(mol·K)
$t$	time, s
$T$	temperature, K

$U_{\text{ref}}$	open-circuit potential, V
$y$	distance from the film/substrate interface, cm
$Y$	dimensionless distance, $y/l$
<b>Greek</b>	
$\alpha_a$	anodic transfer coefficient
$\alpha_c$	cathodic transfer coefficient
$\theta_s$	state-of-charge at $Y = 1$
$\theta^0$	initial state-of-charge
$\sigma$	dimensionless conductivity
$\sigma^0$	initial conductivity, $(\text{ohm}\cdot\text{cm})^{-1}$
$\phi_s$	potential drop across film/electrolyte interface, V
$\Phi_s$	dimensionless potential driving force at $Y = 1$
$\tau$	dimensionless time, $tD_{H^+}/l^2$

## References

- [1] Choi, K. W. and N. P. Yao, **Proceedings of the Symposium on Battery Design and Optimization**, S. Gross (ed.), The Electrochemical Society Inc., Princeton, NJ (1979).
- [2] Micka, K. and I. Roušar, *Electrochim. Acta*, **25**, 1085 (1980).
- [3] Micka, K. and I. Roušar, *Electrochim. Acta*, **27**, 765 (1982).
- [4] Fan, D. and R. E. White, *J. Electrochem. Soc.*, **138**, 17 (1991).
- [5] Fan, D. and R. E. White, *J. Electrochem. Soc.*, **138**, 2952 (1991).
- [6] G. W. D. Briggs, and P. R. Snodin, *Electrochim. Acta*, **27**, 565 (1982).
- [7] Zimmerman, A. H. and P. K. Effa, *J. Electrochem. Soc.*, **131**, 709 (1984).
- [8] Zhang, C. and S. Park, *J. Electrochem. Soc.*, **134**, 2966 (1987).
- [9] Bouet, J., F. Richard, and P. Blanchard, *Proceedings of the Symposium on Nickel Hydroxide Electrodes*, D. A. Corrigan and A. H. Zimmerman, Eds., p. 260, The Electrochemical Society Inc., NJ (1990).
- [10] Sinha, M., *A Mathematical Model for the Porous Nickel Hydroxide Electrode*, Dissertation, University of California, Los Angeles, 1982.
- [11] Mao, Z. R. E. White, and J. Newman, Submitted to, *J. Electrochem. Soc.* (1992).
- [12] Delahay, P., *J. Am. Chem. Soc.*, **75**, 1190 (1953).
- [13] Bender, C. M. and S. A. Orszad, **Advanced Mathematical Methods for Scientists and Engineers**, McGraw Hill, New York, NY (1978).
- [14] Dahlquist, G. and Å. Björk, **Numerical Methods**, Translated by N. Anderson, Prentice Hall, New York, NY (1974).

<u>Parameter</u>	<u>Interpretation</u>	<u>Definition</u>
$\mathcal{D}$	$\frac{\text{discharge time}}{\text{mass-transfer resistance}}$	$\frac{3600n D_{H^+}}{l^2}$
$I_o$	$\frac{\text{discharge time}}{\text{charge-transfer resistance}}$	$\frac{3600n i_o}{F C_{Ni} l}$
$\Theta$	$\frac{\text{discharge time}}{\text{ohmic resistance}}$	$\frac{3600n \sigma_o}{f F C_{Ni} l^2}$

Table 1: The definitions of the dimensionless parameters that govern discharge curves in nickel hydroxide.

$c_{Ni} = 0.040 \text{ mol/cm}^3$	$D_H^+ = 4.6 \times 10^{-11}$
$i_o = 6.0 \times 10^{-3} \text{ A/cm}^2$	$l = 5.0 \times 10^{-4} \text{ cm}$
$\sigma^o = 0.1185 \text{ (ohm}\cdot\text{cm)}^{-1}$	$T = 293 \text{ K}$
$\alpha_a = \alpha_c = 0.5$	$\theta^o = 0.99$

Table 2: Parameters used to obtain Figure 1 [11]. The three dimensionless parameters that result from these values are listed in Figure 1.

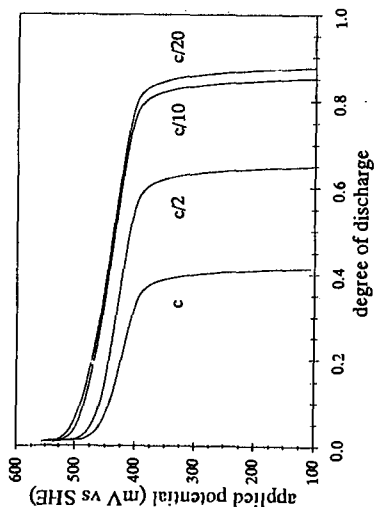


Figure 1: The effect of discharge rate on discharge curves for nickel hydride. The term  $c/n$  is the current which causes the electrode to completely discharge in  $n$  hours. As  $n$  increases the discharge rate decreases. ( $\Theta = 11,380$  h,  $I_a = 11.19$  A,  $D = 0.662$  cm<sup>2</sup>)

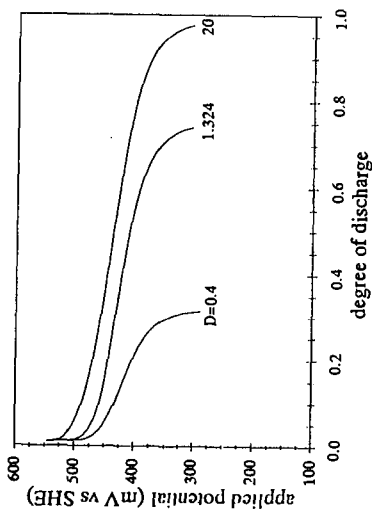


Figure 2: The effect of proton mass-transfer resistance on a  $c/2$  discharge curve. As  $D$  increases, mass-transfer resistance decreases relative to discharge time. ( $\Theta = 2 \times 10^3$ ,  $I_a = 22.38$ )

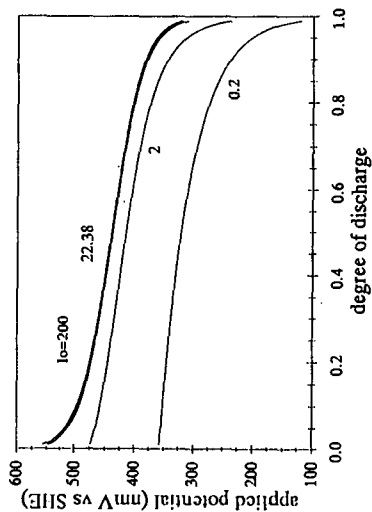


Figure 3: The effect of kinetic resistance on a  $c/2$  discharge curve. As  $I_a$  increases, kinetic resistance decreases relative to discharge time. ( $\Theta = 2 \times 10^3$ ,  $D = 20,000$ )

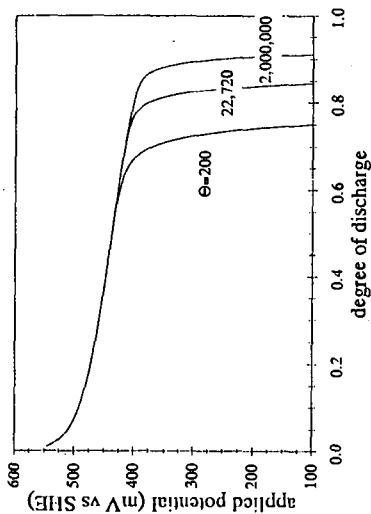


Figure 4: The effect of ohmic resistance on a  $c/2$  discharge curve. As  $\Theta$  increases, the ohmic resistance decreases relative to discharge time. ( $I_a = 22.38$ ,  $D = 20,000$ )